Efficacy of SCMs to mitigate ASR in systems with higher alkali contents assessed by pore solution method

Marie Joshua Tapas[a,*], Lionel Sofia[b], Kirk Vessalas[a], Paul Thomas[a],
Vute Sirivivatnanon[a], Karen Scrivener[b]
[a]University of Technology Sydney, Australia
[b]École Polytechnique Fédérale de Lausanne, Switzerland
*corresponding author: mariejoshua.tapas@uts.edu.au

Abstract

This study demonstrates the efficacy of supplementary cementitious materials (SCMs) to mitigate alkali-silica reaction (ASR) even when used in conjunction with cement of higher alkali contents (up to 1% Na_2O_{eq}). The expansion of concrete prisms was studied immersed in simulated pore solution in order to address the limitations of conventional ASR testing methods, accelerated mortar bar test (AMBT) and concrete prism test (CPT). Expansion results demonstrate that 25% fly ash and 50% slag are both sufficient to mitigate ASR even with cements with alkali content up to 1% Na_2O_{eq} and that the pore solution method is a viable alternative ASR testing method. Massive amounts of ASR products (~20 µm thickness) were observed in concretes without SCMs consistent with high degree of expansion and extensive cracking. Small amounts of ASR products (≤5 µm thickness) were also observed in concrete with SCMs despite absence of significant expansion.

Keywords: alkali-silica reaction; ASR products; pore solution; fly ash; ground granulated blast furnace slag

1. Introduction

Alkali-silica reaction (ASR) is a major concrete durability issue, arising from the dissolution of certain siliceous (SiO_2) components of aggregates and consequent formation of ASR products that results in cracking and loss of serviceability of concrete structures. In alkaline environments (typical of concrete), hydroxyl ions attack the (≡Si-O-Si≡) linkages, resulting in the dissolution of silica network. The negatively charged silicate ions react with available potassium and sodium ions in the pore solution forming alkali silicates [1]. Calcium also participates in the reaction resulting in the formation of the ASR product, alkali calcium silicate hydrate ((N,K)-

C-S-H) [1, 2]. The ASR products formed in confined spaces (i.e. within aggregates) exert pressure on the concrete that can lead to deleterious cracking. Although ASR was first identified by Stanton in 1940 [3], field cases of ASR in Australia were identified only in the 1980s [4]. The 1st case of ASR in Australia is a 36-year-old bridge structure in Perth, Western Australia. The bridge showed severe map cracking and investigation of the cores extracted from the bridge confirmed the presence of ASR products [5]. SA HB 79:2015 (Alkali Aggregate Reaction—Guidelines on Minimising the Risk of Damage to Concrete Structures in Australia) lists some of the other Australian structures affected by ASR [6].

Adding supplementary cementitious materials (SCMs) in concrete mixes is widely recognized as the most practical way of mitigating ASR [7]. SCMs allow the use of aggregates that are otherwise not suitable for concrete structures. In Australia, it is recommended to use 25% fly ash or about 50-65% slag in concrete mixes [6]. The use of SCMs like metakaolin and silica fume is very limited for reasons of cost. Further, adequate dispersion of silica fume during concrete batching is a challenge and typically results in agglomeration of particles that can act as potential sites for ASR [6].

In addition to the use of SCMs, Australian standards impose a limit of 0.6% Na_2O_{eq} (sodium oxide equivalent=$Na_2O + 0.658\ K_2O$) on cement alkali content in order to mitigate ASR. This low alkali limit means that a tremendous amount of raw materials (limestone in particular) is unsuitable for cement production. Since the ability of SCMs to mitigate ASR has long been established, both by accelerated test methods and field exposure studies [7-14], there is then a question as to whether a cement alkali limit is still necessary when SCMs are already included in the concrete mix. Relaxing the cement alkali limit offers the potential not only to reduce costs associated with cement production but also conserve environmental resources.

Standard laboratory test methods such as accelerated mortar bar test (AMBT) and concrete prism test (CPT) are typically employed to assess SCM efficacy in the short term. However, despite worldwide popularity, with several countries having their own version of the tests, AMBT and CPT are both questionable with respect to their ability to assess the effect of cement alkalinity on ASR expansion [15-17]. For ASR testing, Australia uses its own version of these accelerated tests, AS 1141.60.1 (AMBT) and AS 1141.60.2 (CPT) which are very similar to well-known ASTM C1260 and ASTM C1293, respectively [18].

In the AMBT there is an inexhaustible supply of alkalis from the storage solution of 1M NaOH and high temperature of 80 °C. As a consequence, this test has been shown incapable of detecting expansion differences in mortars of varying cement alkali contents [19]. CPT, which is generally accepted as the more reliable test method due to the lower temperature of 38 °C and fixed supply of alkali, is prone to alkali leaching. Hence, boosting to 1.25% Na_2O_{eq} is primarily intended to counteract the leaching. The reported leaching of alkali in concrete prisms for 1 year however ranges from 25-35% [15, 20] and even goes as high as 45% for a 2-year test period [21]. This results in an underestimation of expansion and consequently may indicate lower dosage of SCMs than required for effective mitigation in the field [15, 16, 22, 23]; hence, the many efforts to prevent leaching and improve reliability of the CPT which, to date, remain unresolved [17, 21, 24]. Field studies, which are considered to be the most reliable, take very long time and require not only commitment but also abundant resources. For this reason, most countries, including Australia, do not have field exposure sites at present.

Due to the limitations of existing ASR test methods, this study uses an alternative method to assess the effect of cement alkalinity on the ability of SCMs to mitigate ASR. The test method, developed by the Laboratory of Construction Materials (LMC) at EPFL [25], makes use of simulated pore solutions to assess the efficacy of SCMs to mitigate ASR addressing the leaching issues in CPT and eliminating aggressive test conditions in AMBT (high temperature and excessive supply of alkalis). By studying the expansion of highly reactive aggregates in combination with SCMs (fly ash and slag) using the simulated pore solution method, the aim of this study is to determine if the SCMs at recommended dosages will work to mitigate ASR when used in conjunction with cement which has effective equivalent alkali content of 1% Na_2O_{eq}. The effect of SCM addition on calcium silicate hydrate (C-S-H) composition, alkali uptake in the C-S-H and on the composition of the ASR products are also investigated.

2. Materials and Methods

2.1. Raw Materials

All raw materials (cement, aggregates, SCMs) were sourced in Australia. Cement (Type GP/OPC) and SCMs were supplied by Cement Australia and conform with Australian standards AS 3972 (General Purpose and Blended

Cements), AS 3582.1 (Supplementary Cementitious Materials: Fly Ash) and AS 3582.2 (Supplementary Cementitious Materials: Slag-Ground Granulated Blast Furnace). Two aggregates, a dacite and rhyolite sourced from two Australian quarries, were used in this study. The aggregate suppliers as well as the locations of the quarries are however not possible to disclose as part of confidentiality agreement. The aggregates were supplied both as manufactured sand/fine aggregates (<5 mm) and as coarse aggregates (≥5 to 25 mm). Table 1 lists the X-ray fluorescence (XRF) oxide composition of all the raw materials. The analysis was carried out using PW2400 Sequential WDXRF Spectrometer. The LOI (loss on ignition) was measured on a sub-sample at the same temperature as the fusion beads (1050 ^{o}C). Table 2 shows the mineralogical composition of the aggregates obtained by petrography. The petrographic examination was conducted in accordance with Australian Standards AS2758.1 (1985) and ASTM C-295 (1990) by the Department of Geology, University of Newcastle, Australia.

Table 1 *XRF oxide composition of the raw materials*

Oxide wt%	Cement	Fly Ash	Slag	Dacite	Rhyolite
SiO_2	19.7	59.2	34.1	68.4	61.9
TiO_2	0.2	1.1	0.9	0.4	0.8
Al_2O_3	4.8	28.1	14.4	13.3	15.4
Fe_2O_3	3.1	3.7	0.3	3.3	5.8
Mn_3O_4	0.1	0.1	0.4	0.1	0.1
MgO	0.9	0.5	5.3	1.3	1.6
CaO	64.2	2.5	41.6	2.4	2.3
Na_2O	0.3	0.6	0.4	2.4	5.7
K_2O	0.4	1.2	0.3	3.8	2.9
P_2O_5	0.1	0.4	0.0	0.1	0.2
SO_3	2.4	0.2	2.8	<0.01	0.1
L.O.I.	4.1	1.1	0.4	4.5	4.1
Total	100.2	98.7	100.7	99.9	100.8

Table 2 *Mineralogical composition of the aggregates*

Mineral	Dacite	Rhyolite
Quartz	45%	45%
Feldspar	30%	35%
White mica	10%	5%
Chlorite	5%	5%
Calcite	5%	7%
Magnetite	5%	1%

X-ray diffraction (XRD) patterns of fly ash, slag and cement are shown in Fig. 1 confirming the presence of expected phases [26]. The XRD patterns were obtained on a Bruker D8 Discover XRD in Bragg-Brentano mode using Cu Kα radiation (1.5418 Å) at a scan rate of 0.04 °/second. Phases were identified using DIFFRAC.EVA software and ICDD PDF 4+ database. XRD samples were prepared by front-loading, taking extreme care not to over press the surface to avoid the occurrence of preferred orientation.

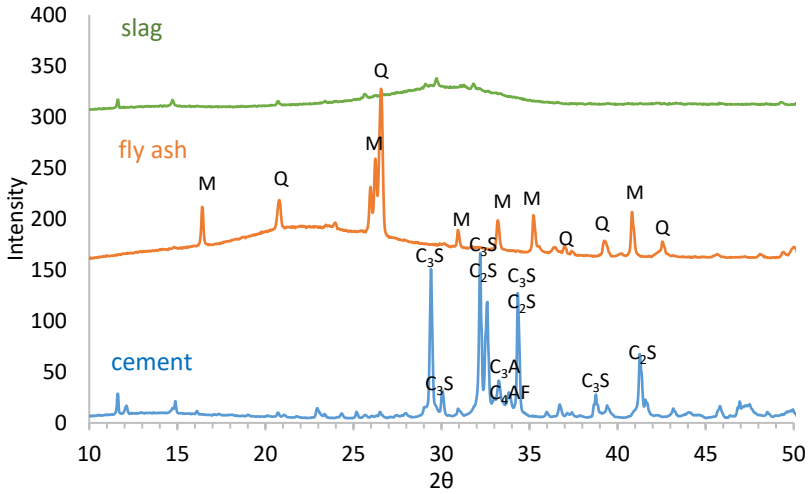

Fig.1. *XRD patterns of cement, fly ash and slag where Q=quartz, M=mullite, C_3S= tricalcium silicate, C_2S=dicalcium silicate, C_3A=tricalcium aluminate and C_4AF=tetracalcium alumina ferrite*

2.2. Preparation of the Concrete Prisms

Concrete prisms (70 x 70 x 280 mm) with cement content of 410 kg/m^3 were cast using Australian reactive aggregates, SCMs and cement. 3 concrete prisms were prepared for each mix using the same type of aggregate for both fine and coarse components (0.16 µm- 22.4 mm aggregate sizes) keeping the water to cement ratio at 0.46 for all mixes. Table 3 shows the aggregate grading used for the concrete prisms. To simulate a cement with 1% Na_2O_{eq} alkali content, the cement with original 0.6% Na_2O_{eq} was boosted with 0.4% extra alkali by adding sodium hydroxide (NaOH) to the mixing water. The alkali was added based on the cement content and not the binder content. The SCMs were used at Australian recommended dosages for effective mitigation, 25% for fly ash and 50% for slag. Table 4 lists the mix designs investigated.

The concrete prisms were demoulded after 24±2 hours and left to cure for 28 days in a high humidity environment (fog room), at 20±2 °C before being stored in simulated pore solution at 60 °C. The 28 days curing is to allow the concrete to develop strength. This is in contrast to 1 day curing prescribed in ASTM C1293.

Table 3. *Aggregate grading*

Grain Size	%
0.16-0.32	5
0.32-0.63	5
0.63-1.25	5
1.25-2.50	10
2.50-5.00	15
5.00-8.00	15
8.00-12.50	20
12.50-22.40	25

Table 4 *Mix designs for concrete prisms in kg/m^3*

Concrete Mixes	Aggregates (kg/m^3)		Cementitious Materials (kg/m^3)			water (kg/m^3)	*NaOH added (kg/m^3)	Effective cement alkali content (Na_2O_{eq})
	Rhyolite	Dacite	OPC	slag	fly ash			
Density (kg/m^3)	2700	2660	3150	2900	2100	1000	-	-
RY No SCM	1795	0	410	0	0	190	0	0.60%
RY+25%FA+0.4%Alkali	1750	0	310	0	100	190	1.6	1.00%
RY+50%SL+0.4%Alkali	1780	0	205	205	0	190	1.1	1.00%
DC No SCM	0	1770	410	0	0	190	0	0.60%
DC+25%FA +0.4%Alkali	0	1725	310	0	100	190	1.6	1.00%
DC+50%SL +0.4%Alkali	0	1755	205	205	0	190	1.1	1.00%

**the conversion of Na_2O_{eq} to NaOH has been taken into account ($Na_2O + H_2O = NaOH$)*

2.3. Preparation of the Simulated Pore Solution and ASR Expansion Monitoring

Pastes with equivalent composition and water to cementitious material ratio as the concrete prisms were prepared in sealed containers and cured for 28 days under high humidity environment at 20±2 °C. Additional pastes with SCMs but no alkali boosting and with SCMs + 0.2% alkali boosting were also prepared. Similar to the concrete prisms, alkali boosting was carried out by adding NaOH to the mixing water. The paste samples were shaken slowly a few times after casting to prevent settlement and bleeding before setting. Consequently, no bleed water was observed in any of the hardened pastes.

Pore solution was extracted from the pastes at 28 days using 1500 kN force (equivalent to applied stress of 764 MPa) in a compression testing machine. The extracted solutions were filtered with 0.2 µm membrane to remove solid residues and then analysed by inductively coupled plasma optical emission spectroscopy (ICP-OES) to determine the concentration of elements, Ca, Al, Si, Na and K in the pore solution. The extracted pore solutions were diluted 3 times with de-ionised water and acidified with 120 µL of high purity nitric acid. ICP-OES analysis was carried out using Shimadzu ICPE-9000 at the Central Environmental Laboratory, EPFL. The concentration of elements in the pore solution was measured at 10, 100 and 1000 times dilution of the original sample.

The simulated pore solutions used to store the concrete prisms (Table 5) were then prepared based on the alkali content (Na and K concentration) of the paste system corresponding to the binder of the concrete at 28 days. Analytical grade NaOH and KOH pellets and high purity water were used to prepare the storage solutions. The other elements (Ca, Al and Si) were found to have very low concentration and hence, were not included in the preparation of the simulated pore solution. Another set of pastes cast from the same mix as the 28 day pastes were also subjected to pore solution extraction after 6 months (168 days) in order to monitor the effect of time on the stability of the pore solution.

Table 5 *Storage solutions for the concrete mixes*

Concrete Mix	**Storage Solution (mol/L)**		
	Sodium (Na)	**Potassium (K)**	**Na+K**
Rhyolite No SCM	0.18	0.27	0.45
Rhyolite +25%FA +0.4% Alkali	0.32	0.14	0.46
Rhyolite +50%SL + 0.4% Alkali	0.25	0.10	0.35
Dacite No SCM	0.18	0.27	0.45
Dacite +25%FA + 0.4% Alkali	0.32	0.14	0.46
Dacite +50%SL + 0.4% Alkali	0.25	0.10	0.35

ASR expansion measurements were obtained using a vertical comparator before immersing the concrete prisms in the storage solution (zero hour expansion reference) and every 28 days to monitor expansion. The concrete prisms were stored at 60 °C in a climate chamber. For expansion measurements, the concrete prisms were taken out of the climate chamber 1 day prior measurement to cool to room temperature as this ensures that the concretes are in similar conditions and therefore reduce measurement errors.

2.4. Characterization of ASR Products and C-S-H Composition

At 6 months (168 days), part of the concrete specimens were sectioned for microstructural analysis. The concrete was cut using a diamond saw to make 4cm x 4cm x 1cm (L x W x H) specimens. These were rough polished to obtain 3cm x 3cm x 1cm specimens (biggest mould dimension) and minimise damage induced by cutting. The free water was removed by immersing the cut concrete in isopropanol for 7 days (solvent exchange process). After which, the specimens were vacuum impregnated with epoxy resin (Epotek-301) and then polished. The samples were first polished with sandpaper grade 500 and 1200, respectively, until the sample surface had been fully uncovered from the resin, followed by automated polishing using MD Largo Struers discs lubricated with petrol and diamond spray as a polishing agent (9 µm, 3 µm and 1 µm particle sizes). After polishing, the samples were cleaned in an ultrasonic bath for 2 minutes and then stored in a vacuum desiccator for at least 2 days to dry. The samples were coated with carbon to prevent charging during SEM imaging.

Imaging and elemental analysis of the carbon-coated polished sections were carried out using FEI Quanta 200 with Bruker XFlash 4030 EDS detector. The microscope was operated in backscattered electron (BSE) mode, 15 kV accelerating voltage and 12.5 mm working distance in high vacuum ($<5x10^{-5}$ mbar). To ensure consistent beam current, X-ray intensities from a copper foil placed on the metallic sample holder was measured before each analysis point. The spot size (typically around 5.0) is adjusted until a specified system factor is reached. The system factor, which is kept constant for all EDS analyses, serves as the indirect measure of current as the equipment does not allow direct current measurement. Increasing the spot size, increases the current. With the optimized conditions, it takes only 3 seconds (50,000 counts) to analyse each point. This minimizes damage to the hydrates while providing sufficient statistics for the spectrum. A predefined list of elements (O, Na, Mg, Al, Si, P, S, Cl, K, Ca, Ti, Fe) was used for identification and quantification using $\varphi(\rho z)$ correction.

The composition of C-S-H was measured by point EDS analysis on the hydration rims around the hydrated clinker (inner C-S-H). The analyses were carried out on 'inner-C-S-H' because it is considered to be relatively homogeneous compared to the 'outer-C-S-H' which is finely intermixed with other hydration products (mainly aluminates) [27]. A minimum of 200 points were analysed per sample. Elemental mapping (EDS mapping) was

also carried out to better illustrate the distribution of elements in the ASR products. Mapping was carried out using similar parameters as point EDS but with longer signal acquisition time of 20 minutes.

3. Results and Discussion

3.1. Pore Solution Extracted from Blended Pastes (28 days and 168 days)

Figs. 2 and 3 show the concentration of different elements (Al, Ca, K, Na, Si) in the extracted pore solution at 28 days. The reported concentrations are in agreement with other studies that despite the alkalis being a very small percentage of the cement, they dominate the pore solution [7, 28, 29]. Whereas, K concentration ranges from 0.10 to 0.27 mol/L and Na from 0.12 to 0.32 mol/L, other elements Ca, Al, and Si all have concentration lower than 0.003 mol/L. As the concentration of other elements are minor, only the alkali contents were considered for the simulated pore solution. It is however worth noting from Fig. 3 that aluminium in the pore solution increases with SCM addition, with 50% slag blended pastes demonstrating much higher aluminium contents in the pore solution than 25% fly ash blended pastes.

Adding SCMs, in this case 25% fly ash or 50% slag, lowers the pore solution alkali concentration (Na and K). 50% slag notably lowers the alkali concentration more than 25% fly ash. The effect of alkali boosting (by NaOH addition) can also be observed with Na concentration increasing with increasing level of boosting (from 0.2% to 0.4%). The effect of SCM addition on pore solution alkali concentration is a combined effect of cement dilution and alkali binding in the calcium silicate hydrate (C-S-H). This is generally accepted as the main mechanism of ASR mitigation by SCMs [8, 26, 30-32]. Incorporating SCMs in the concrete mix, modifies the Ca/Si ratio as well as the Al/Si ratio of the C-S-H phases. This modification is responsible for the increase in the alkali binding capacity of the C-S-H when SCMs are present [7, 33, 34]. The effect of fly ash and slag on C-S-H composition and alkali uptake is discussed in Section 3.4.

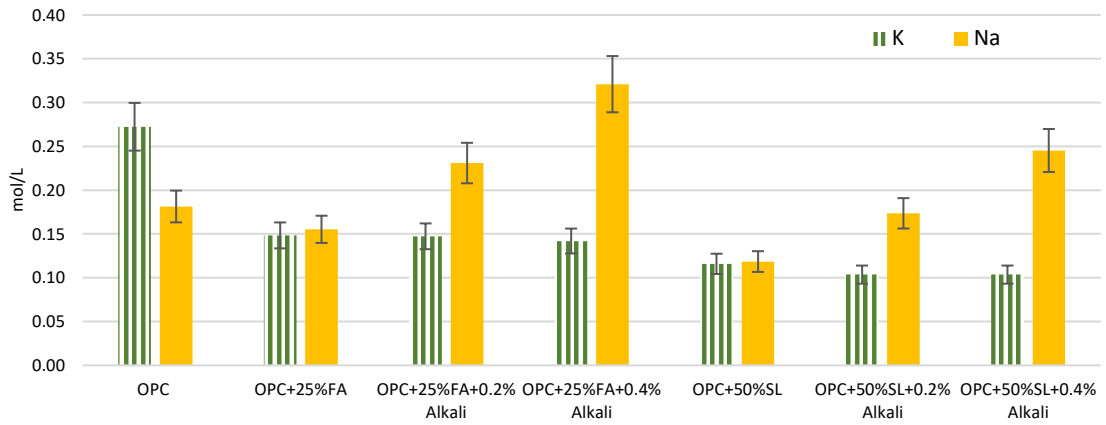

Fig. 2. *Concentration of sodium (Na) and potassium (K) in the pore solution at 28 days*

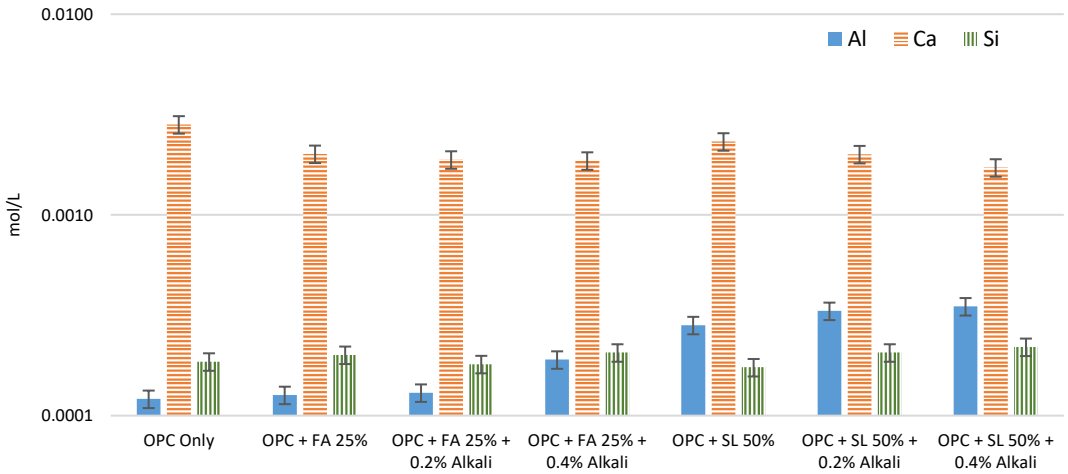

Fig. 3. *Plot of log of the concentration of aluminium (Al), calcium (Ca) and silicon (Si) in the pore solution at 28 days*

Fig. 4 shows the effect of age on the pore solution alkali concentration. For OPC, a slight increase in the concentration of Na+K from 28 days to 168 days can be observed. The increase in the concentration of Na and K in OPC with time was reported in several studies [28, 29, 35]. The alkali concentration increases with time as alkalis continue to be released during the hydration of clinkers and as the volume of the liquid phase decreases [35]. For the pastes with SCMs, in general, small further decreases in alkali concentration were observed after 168 days. The decrease can be attributed to SCM reactions and alkali binding in the hydration products [7]. For fly ash, the decrease is quite substantial indicating that the use of 28 days pore solution is conservative. However, considering the error in measurement, the small differences observed from 28 to 168

days confirm that the pore solution concentration is fairly stable after 28 days and this therefore validates the use of 28 day extracted pore solution as a storage solution in the current method.

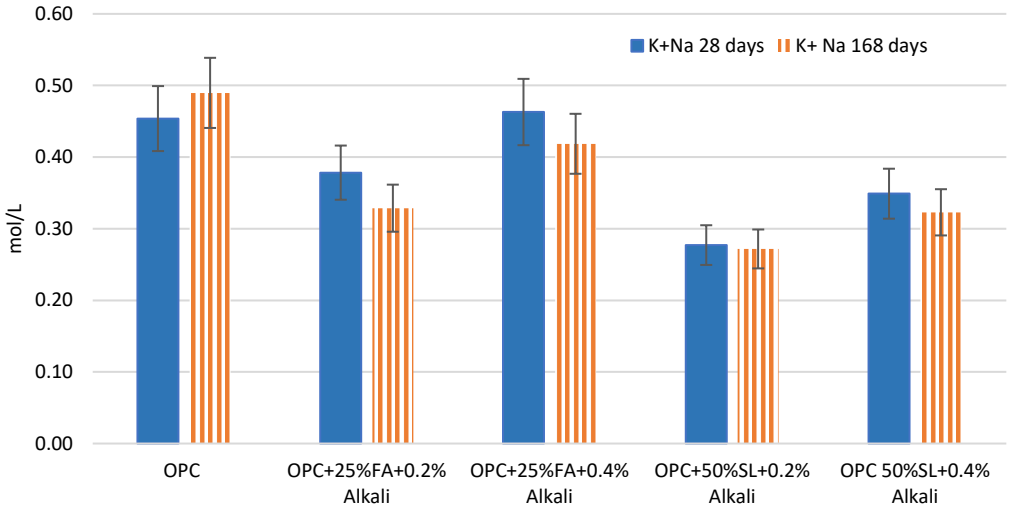

Fig. 4. *Effect of age on total alkali concentration in the pore solution*

3.2. ASR Expansion Data (Simulated Pore Solution Method)

Fig. 5 shows the expansion data up to 1 year for the concrete prisms. Whereas, the prisms with no SCMs have expanded considerably (both aggregates), the prisms with SCMs (25% fly ash or 50% slag) even with cement boosted with 0.4% alkali (1% effective Na_2O_{eq}), do not show significant expansion. Therefore, the results clearly demonstrate that the SCMs at Australian recommended dosages can potentially mitigate ASR even with cements of higher alkali contents. It is also worth noting that the expansion of Dacite concrete without SCM at 1 year is slightly higher than the Rhyolite concrete, although overall, the expansion rates are almost comparable which may be due to their similar mineralogical composition (Table 2).

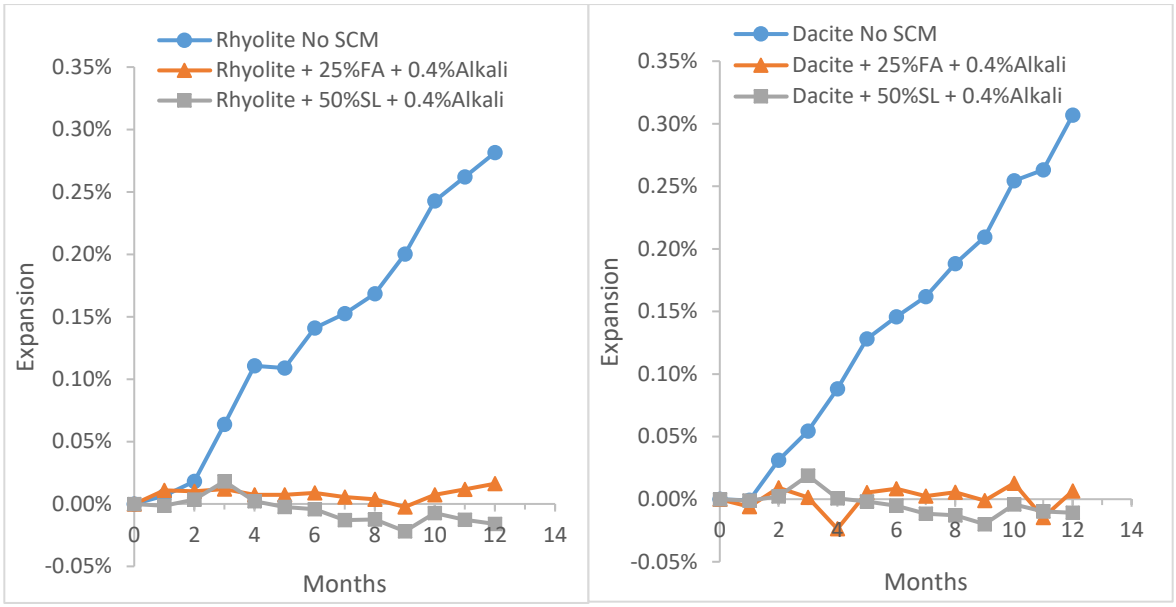

Fig. 5. *Measured expansion of the concrete specimens stored at 60 °C*

The expansion results are consistent with some field studies that confirmed the efficacy of SCMs when used in conjunction with high alkali cement [15, 36-38]. The Lower Notch Dam in Ontario Canada made use of highly reactive greywacke-argillite coarse aggregates and high alkali cement (1.08% Na_2O_{eq}) in combination with 20% to 30% low CaO fly ash has shown no indications of ASR damage after more than 40 years in service [15, 36, 39]. Fly ash used at replacement levels of 25% and 40% was sufficient to inhibit both expansion and cracking in concrete blocks containing alkali-silica reactive aggregates, and high alkali cement (K_2O= 1.10%, Na_2O= 0.43%) in an outdoor exposure site in England for a period of up to 18 years [38]. Moreover, 50% slag used in concrete made with high-alkali cement (> 0.8%) and reactive Spratt aggregate also showed no sign of ASR or cracking after 20 years. Equivalent concrete with high alkali cement but no SCM cracked after 5 years [37].

3.3. Morphology and Composition of the ASR Products

The concrete specimens were sectioned to analyse the ASR products. Extensive cracking was observed in concrete specimens with no SCMs as can be seen from Figs. 6 and 7. The ASR product appears to originate from the interior of the aggregate extending towards the cement paste. Its appearance and location are consistent with that reported in literature [40-42]. Some cracks were found to not contain ASR products and may be a result of expansion due to the formation of ASR products in other parts of the aggregate [40, 42].

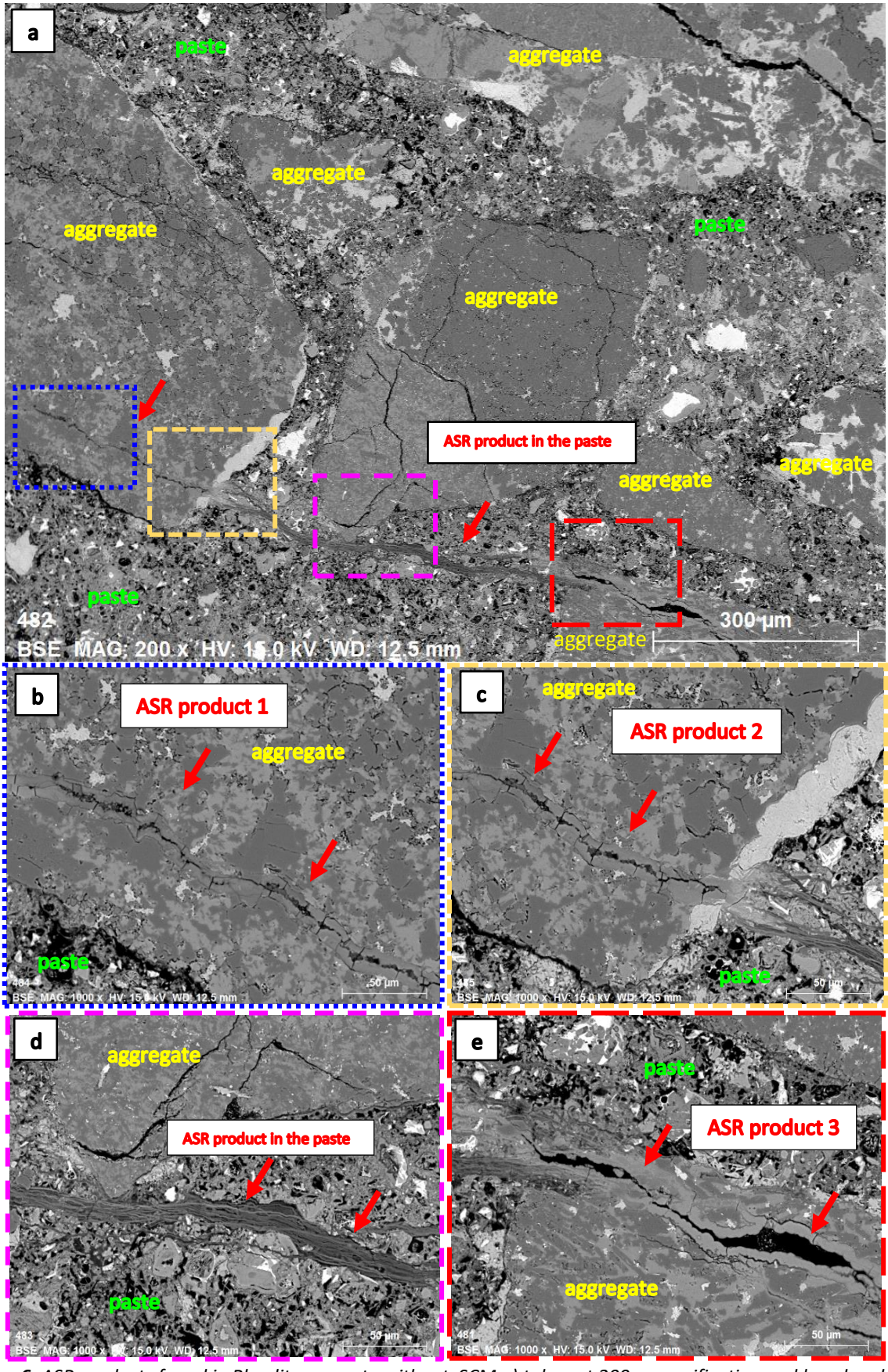

Fig. 6. *ASR products found in Rhyolite concrete without SCM a) taken at 200x magnification and b,c, d and e) at higher magnification of 1000x*

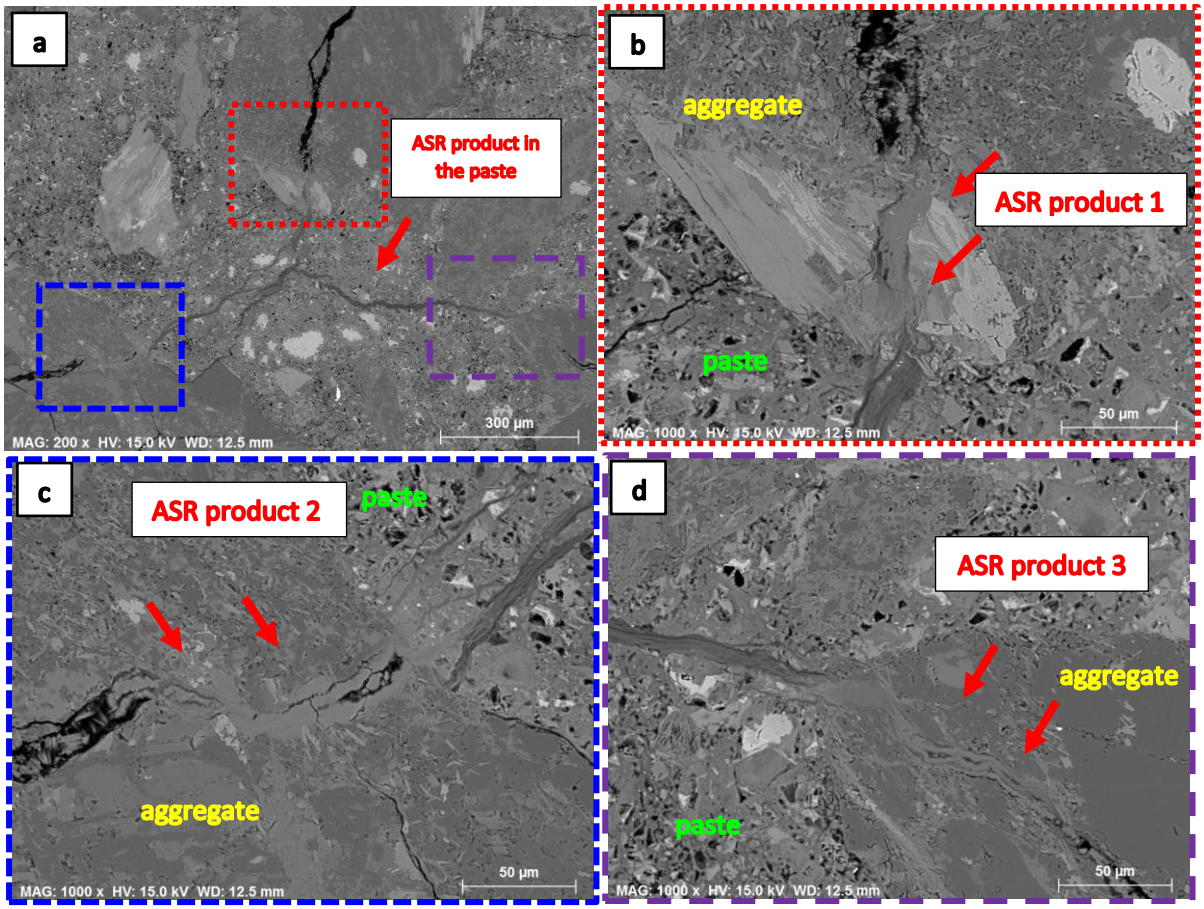

Fig. 7. *ASR products found in Dacite concrete without SCM a) taken at 200x magnification and b,c and d) at higher magnification of 1000x*

EDS map of the ASR product in Dacite concrete without SCM shown in Fig. 8 confirm the presence of calcium and alkalis (Na and K). The presence of calcium (Ca) is consistent with the ASR product being alkali calcium silicate hydrate [2, 40-43]. Essentially, calcium is able to precipitate the dissolved silicate species in solution. The actual role of calcium however is still not fully understood. Although higher calcium contents in the ASR product reportedly results in higher stiffness [44], as the ASR product becomes more rigid, it also decreases its swelling potential [2, 45].

Table 6 shows the elemental composition of the ASR products in concrete without SCM depicted in Figs. 6 and 7. Each reported value corresponds to an average of 10-15 EDS points. The Ca/Si ratio (0.29-0.34) and (Na+K)/Si ratio (0.30-0.37) of the ASR products found within the aggregate agrees with that reported in other studies [40, 43, 46, 47]. No significant difference was noted in the composition of the ASR products from the two types of aggregates. The ASR product traversing through the cement paste (Fig. 6d) was however found to have higher

Ca/Si ratio of 1.26 and lower (Na+K)/Si of 0.11 similar to C-S-H [27, 32, 47-49]. Several studies have also reported that the composition of the ASR products varies as a function of its location in the concrete. In general, the silicon content of the ASR product decreases and calcium content increases as it moves closer in contact with the cement paste [42, 47, 49-51]. The change in composition occurs because there is abundant calcium in the pore solution (due to portlandite). Since the calcium replaces the alkali in the ASR product, a much lower alkali content in the ASR product with increasing calcium content is expected [52]. This is consistent with earlier studies which cited lower alkali contents in the ASR products located in the cement paste area [40, 47, 49]. This also agrees with observations in the current study where the high alkali concentration terminates close to the aggregate edge and does not extend towards the paste (Fig. 8).

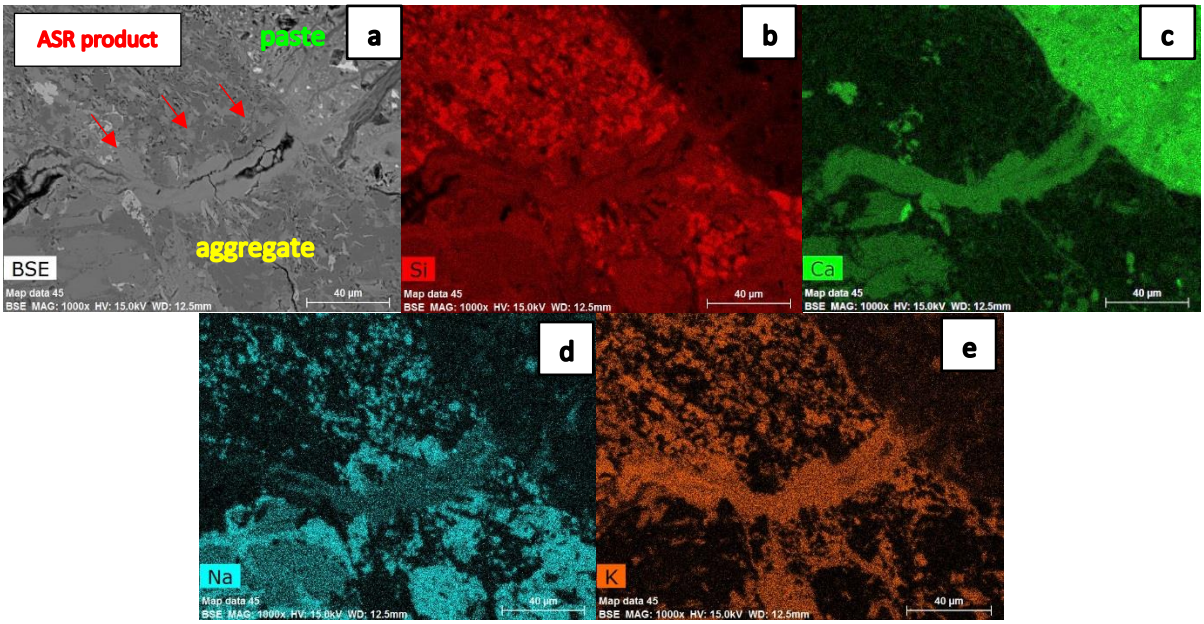

Fig. 8. *EDS map of the a) ASR product within an aggregate in Dacite concrete without SCM confirming presence of b) silicon (Si), c) calcium (Ca), d) sodium (Na) and e) potassium (K)*

In the concrete with SCMs it was also possible to find, very occasionally, deposits of ASR products despite having no significant expansion (Fig. 9). The cracking observed for concrete with SCMs was also significantly less compared to concrete prisms without SCM. Moreover, as can be observed from Fig. 9, the crack width is much narrower, with thicknesses typically of maximum 5 µm in contrast to the veins of about 20 µm in concrete with no SCMs (Figs. 6 and 7). EDS map in Fig. 10 confirm that the main constituents of ASR products in concrete with SCMs are also Si, Ca, K and Na. Spot EDS analysis for the ASR products in concretes containing SCMs is, however, not reported due to the size of the ASR products (≤5 µm), which may lead to potential intermixing with adjacent phases.

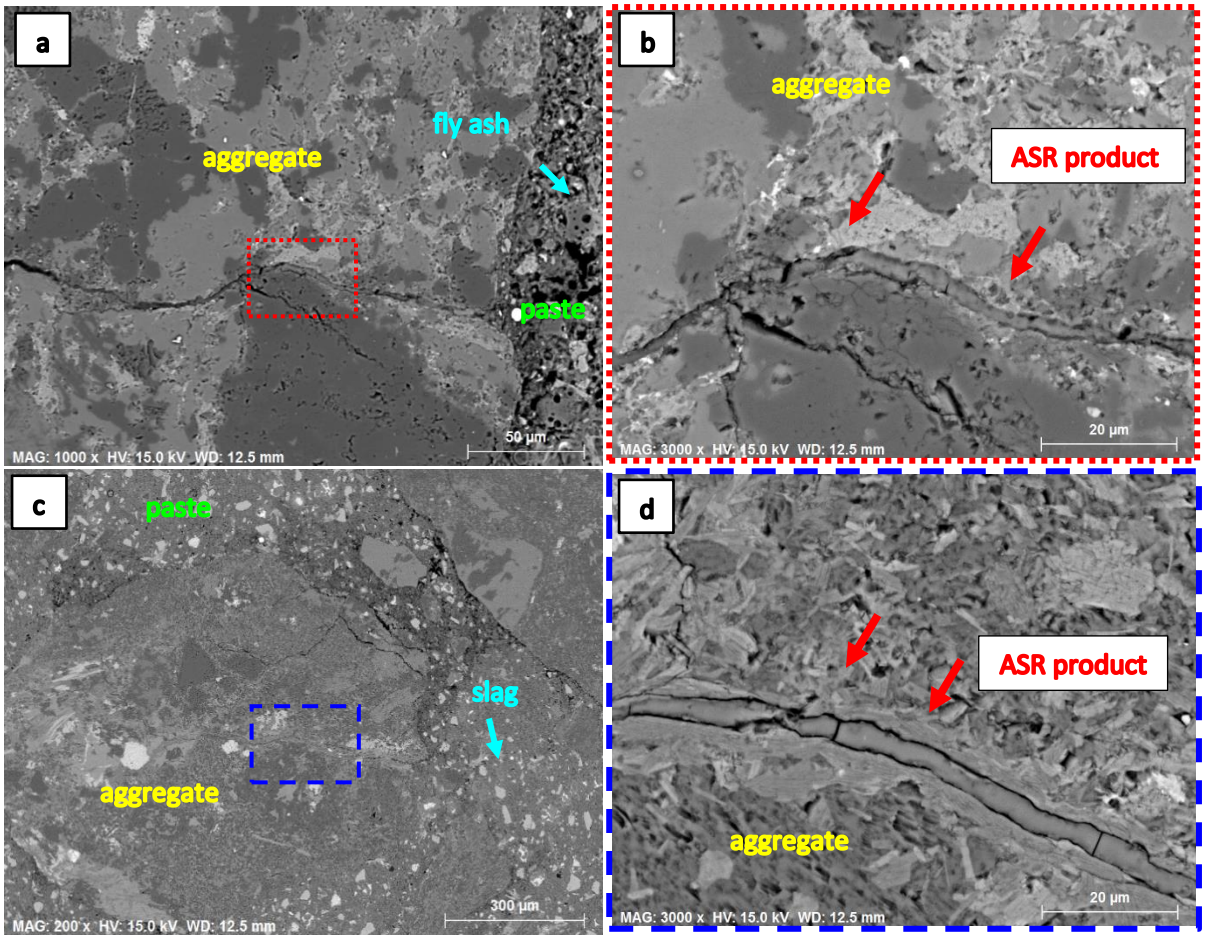

Fig. 9. *ASR products observed in concrete with SCMs a, b) RY +25% FA + 0.4% Alkali and c, d) DC + 50% SL + 0.4% Alkali*

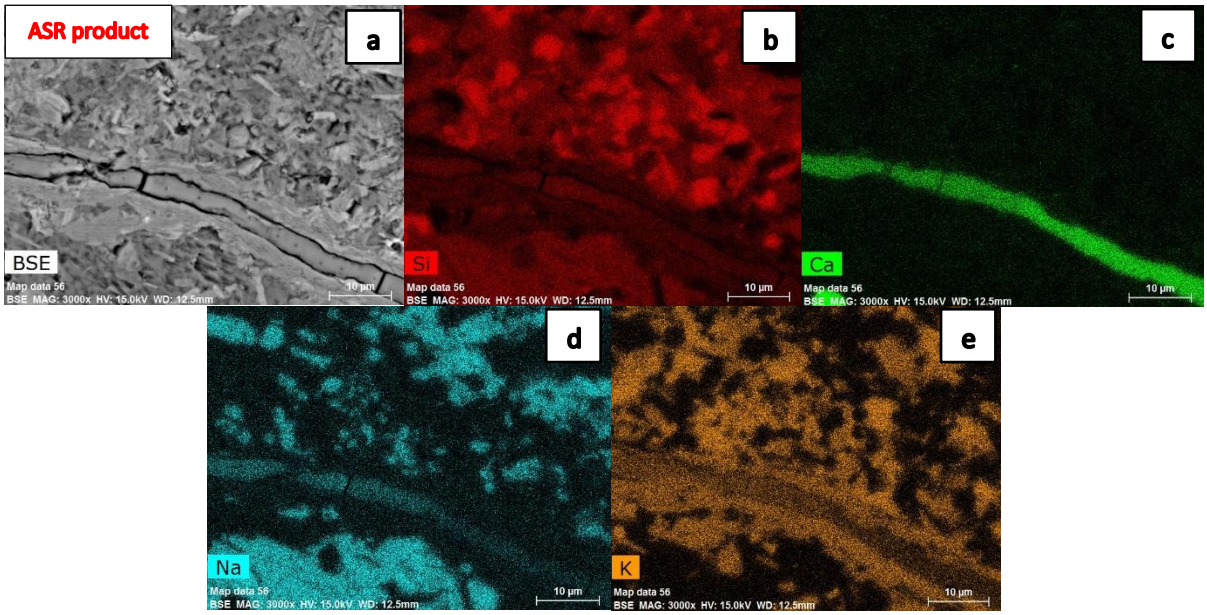

Fig. 10. *EDS map of the a) ASR product within an aggregate in Dacite concrete with 50% slag and 0.4% alkali boosting confirming presence of b) silicon (Si), c) calcium (Ca), d) sodium (Na) and e) potassium (K)*

Table 6 *EDS composition of the ASR products in concrete without SCM (normalized without oxygen)*

ASR product location		Elements (atomic wt%)							
		Ca	Si	Al	Na	K	Na+K	Ca/Si	(Na+K)/Si
Rhyolite No SCM	ASR product 1	18.03	61.87	1.32	7.27	11.51	18.78	0.29	0.30
	ASR product 2	19.53	60.96	1.04	6.60	11.88	18.48	0.32	0.30
	ASR product 3	19.21	60.60	1.20	6.82	12.17	18.99	0.32	0.31
	ASR product in the paste	50.79	40.28	4.63	3.03	1.27	4.30	1.26	0.11
Dacite No SCM	ASR product 1	18.03	59.04	1.14	8.50	13.29	21.79	0.31	0.37
	ASR product 2	20.00	58.31	0.81	6.54	14.34	20.88	0.34	0.36
	ASR product 3	18.87	59.04	1.06	7.95	13.08	21.03	0.32	0.36

3.4. Effect of SCM on C-S-H Composition and Alkali Uptake in the C-S-H

Fig. 11 shows the effect of SCM addition on the C-S-H composition. EDS scatter plots show that the concrete with SCMs (regardless of aggregate type) exhibit higher Si/Ca and Al/Si ratios than concrete with no SCMs. This result is consistent with studies of fly ash and slag blended pastes which reported increase in Si/Ca and Al/Si ratio with increasing SCM replacement levels [34, 53, 54].

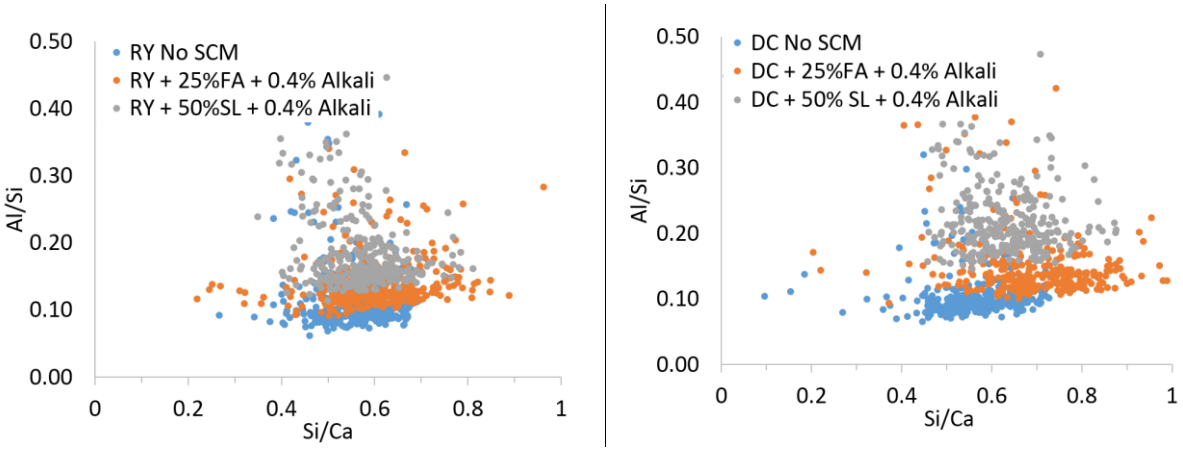

Fig. 11. *Effect of fly ash and slag addition on the Al/Si and Si/Ca of the C-S-H*

The addition of 25% fly ash and 50% slag results in almost equivalent Si/Ca ratio. However, the 50%SL concrete showed higher Al/Si ratios that the 25%FA concrete. This observation is consistent with slightly elevated concentrations of aluminium in the pore solution of 50% slag than 25% fly ash blended pastes reported in Fig. 3. Due to the ASR mitigating effects of aluminium [48, 55, 56], the higher Al/Si ratio in 50% slag concrete therefore suggests that its effect on ASR mitigation may be more in the long term than 25% fly ash concrete.

The modification of C-S-H composition with SCM addition affects the alkali uptake as shown in Fig. 12. The plots clearly demonstrate that SCM addition increases the amount of alkali (Na+K) in the C-S-H. C-S-H phases with higher Si/Ca ratio have higher alkali binding capacity [31, 33, 57]. There is no notable difference in the alkali uptake of concrete with 25% fly ash or 50% slag and this is possibly because of their comparable Si/Ca ratio.

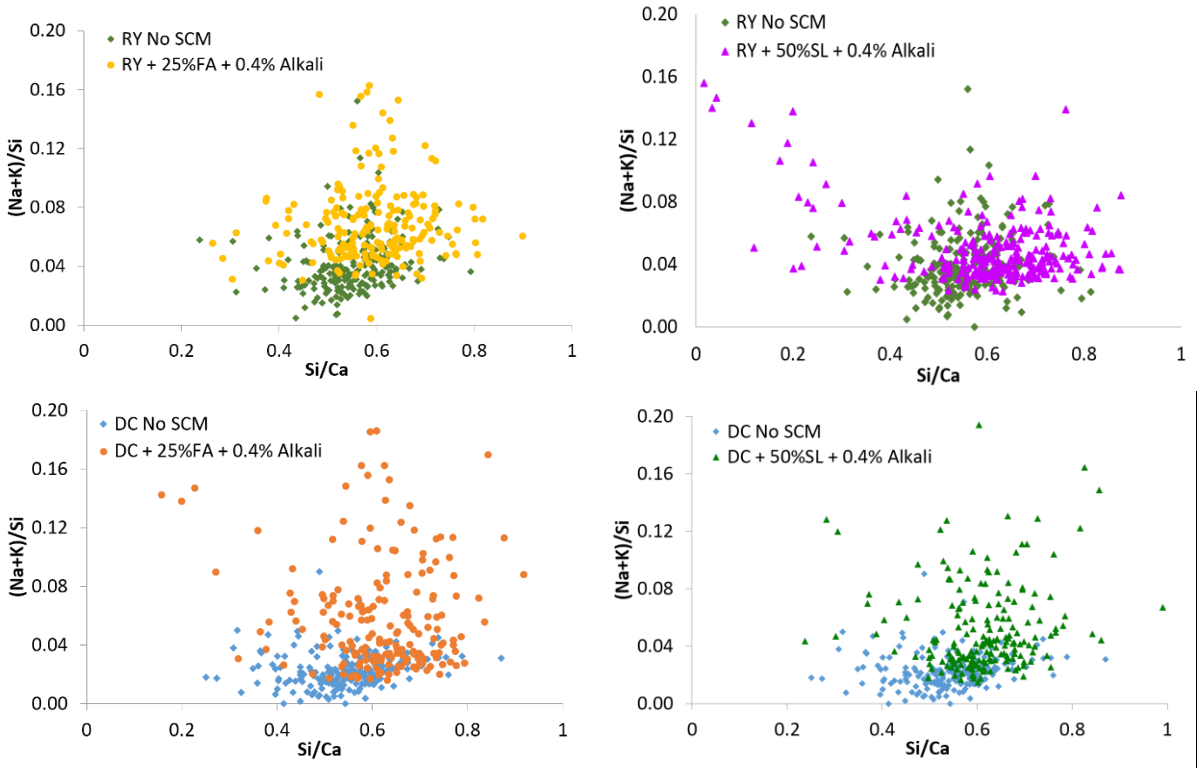

Fig. 12. *Effect of SCM addition on the alkali uptake in the C-S-H*

.

4. Conclusions

This study investigated the efficacy of Australian SCMs to mitigate ASR when the effective cement alkali content was raised to 1% Na_2O_{eq} from original alkali content of 0.6% Na_2O_{eq}. To avoid excessive alkali associated with AMBT, and leaching in CPT, simulated pore solution prepared based on the pore solution alkali concentration at 28 days was used as the storage solution. Extracted pore solution after 168 days (6 months) of pastes cast from the same mix as the 28 day samples confirm that pore solution alkali concentration is fairly stable from 28 days.

370 The expansion results show that, whereas, the concretes with no SCM have significant expansion after 1 year at
371 60 °C, the concrete mixes with SCMs (either 25% fly ash or 50% slag) have no expansion up to 1 year. Results
372 therefore suggest that the SCM dosages used are sufficient to mitigate ASR even at higher cement alkali
373 contents. Moreover, the results also demonstrate that the simulated pore solution method is a viable alternative
374 ASR testing method.
375
376 The concretes were sectioned at 6 months in order to characterize the ASR products and the C-S-H phases.
377 Massive cracking was observed in the concretes without SCM. ASR products (~20 µm thickness), which appear
378 to originate from the aggregate interior and extend towards the cement paste, were also observed extensively.
379 The concretes with SCMs, although did not manifest expansion, also showed the presence of small amounts of
380 ASR products in thin cracks. The composition of the ASR products inside an aggregate in concretes without SCM
381 is comparable regardless of type of aggregate and agrees to that reported in other studies. The elemental
382 composition of ASR products in concrete with SCMs were no longer reported due the size of the ASR
383 products (≤5 µm thickness) which can potentially lead to intermixing with adjacent phases. From the EDS maps
384 however, it is clear that the main constituents are also Si, Ca, Na and K which is comparable to the ASR products
385 in concretes with SCMs. The composition of the ASR products in concretes with SCMs may potentially provide
386 more insights into the mechanisms of ASR mitigation and thus, for future work, the authors propose to use more
387 advanced characterization techniques to quantify the composition of thin ASR products observed in these
388 concretes.
389
390 The C-S-H composition was observed to shift with SCM addition (fly ash or slag) towards increasing Si/Ca and
391 Al/Si ratio. Alkali uptake in the C-S-H increased with SCM addition. Whereas, the effect of 25% fly ash and 50%
392 slag on Si/Ca ratio are almost equivalent, 50% slag increased the Al/Si ratio more than 25% fly ash. Since
393 aluminium has been reported to have added benefit in ASR mitigation due to its ability to prevent dissolution of
394 silica components of aggregates as well as its incorporation in the C-S-H leading to better alkali retention, this
395 suggests that in the long term, 50% slag may have better mitigating capabilities than 25% fly ash.
396
397 This paper reports on the initial 60 °C expansion results and the expansion is being continuously monitored.
398 Moreover, another set of concrete prisms have also been exposed at 38 °C, but in this case the reference samples

have not yet expanded significantly. Hence, the effect of lower temperature as well as levels of alkali boosting on ASR products and C-S-H composition will be reported subsequently.

The longer-term expansion monitoring as well as assessing the expansion of the concrete prisms at 38 °C are expected to provide more information as the boosting of alkali (NaOH) in the proposed test method was carried out in order to simulate an increase in cement alkalinity and not to accelerate the ASR expansion like in traditional CPT which raises the binder alkalinity to 1.25% Na_2O_{eq}. Put simply, since the simulated pore solution method at 60 °C is accelerated only by temperature and not by alkali, longer-term monitoring may be required to see the full extent of expansion and mitigation. Moreover, as the pore solution method is a new ASR test method being proposed, more data is necessary to be able to qualify its effectiveness against traditional test methods and establish expansion test limits.

Declaration of Competing Interest

The authors declare that they have no known competing financial interests or personal relationships that could have appeared to influence the work reported in this paper.

Acknowledgements

This research is supported by an Australian Government Research Training Program Scholarship and is part of the alkali-silica reaction research funded through Australian Research Council (ARC) Research Hub for Nanoscience Based Construction Materials Manufacturing (NANOCOMM) with the support of the Cement Concrete and Aggregates Australia (CCAA). Likewise, the work would not have been possible without the facilities and equipment provided by Laboratory of Construction Materials, EPFL.

References

[1] L.D. Glasser, N. Kataoka, The Chemistry of Alkali-Aggregate Reaction, Cem. Concr. Res., 11 (1981) 1-9.

[2] F. Rajabipour, E. Giannini, C. Dunant, J. Ideker, M. Thomas, Alkali–silica reaction: Current understanding of the reaction mechanisms and the knowledge gaps, Cem. Concr. Res., 76 (2015) 130–146.

[3] T.E. Stanton, Expansion of Concrete through Reaction between Cement and Aggregate, Proc. Am. Soc. Civil Eng., 66 (1940) 1781-1811.

[4] A. Shayan, The current status of AAR in Australia and mitigation measures, Concrete in Australia, 41 (2015) 44-51.

[5] A. Shayan, C.J. Lancucki, Alkali-Aggregate Reaction in the Causeway Bridge, Perth, Western Australia, in: P.E. Grattan-Bellew (Ed.) 7th International Conference on Alkali-Aggregate Reactions, Noyes Publications, Ottawa, Canada, 1986, pp. 392-397.

[6] Standards Australia, Alkali Aggregate Reaction—Guidelines on Minimising the Risk of Damage to Concrete Structures in Australia, SAI Global Limited, Sydney, Australia, 2015.

[7] M. Thomas, The effect of supplementary cementing materials on alkali-silica reaction: A review, Cem. Concr. Res., 41 (2011) 1224–1231.

[8] B. Durand, J. Berard, R. Roux, J. Soles, Alkali-Silica Reaction: The Relation Between Pore Solution Characteristics and Expansion Test Results, Cem. Concr. Res., 20 (1990) 419-428.

[9] A.M. Boddy, R.D. Hooton, M.D.A. Thomas, The effect of the silica content of silica fume on its ability to control alkali–silica reaction, Cem. Concr. Res., 33 (2003) 1263–1268.

[10] T. Ramlochan, M. Thomas, K.A. Gruber, The effect of metakaolin on alkali-silica reaction in concrete, Cem. Concr. Res., 30 (2000) 339-344.

[11] D.W. Hobbs, Deleterious expansion of concrete due to alkali-silica reaction: influence of pfa and slag, Mag. Concr. Res., 38 (1986) 191-205.

[12] M.H. Shehata, M.D.A. Thomas, The effect of fly ash composition on the expansion of concrete due to alkali-silica reaction, Cem. Concr. Res., 30 (2000) 1063-1072.

[13] J. Duchesne, M.-A. Berube, Long-term effectiveness of supplementary cementing materials against alkali–silica reaction, Cem. Concr. Res., 31 (2001) 1057–1063.

[14] Rasheeduzzafar, S.E. Hussain, Effect of microsilica and blast furnace slag on pore solution composition and alkali-silica reaction, Cem. Concr. Compos., 13 (1991) 219-225.

[15] M. Thomas, B. Fournier, K. Folliard, J. Ideker, M. Shehata, Test methods for evaluating preventive measures for controlling expansion due to alkali–silica reaction in concrete, Cem. Concr. Res., 36 (2006) 1842–1856.

[16] J. Lindgård, Ö. Andiç-Çakır, I. Fernandes, T. Rønning, M. Thomas, Alkali–silica reactions (ASR): Literature review on parameters influencing laboratory performance testing, Cem. Concr. Res., 42 (2012) 223–243.

[17] J. Lindgård, M.D.A. Thomas, E.J. Sellevold, B. Pedersen, Ö. Andiç-Çakır, H. Justnes, T.F. Rønning, Alkali–silica reaction (ASR)—performance testing: Influence of specimen pre-treatment, exposure conditions and prism size on alkali leaching and prism expansion, Cem. Concr. Res., 53 (2013) 68-90.

[18] V. Sirivivatnanon, J. Mohammadi, W. South, Reliability of new Australian test methods in predicting alkali silica reaction of field concrete, Constr. Build. Mater., 126 (2016) 868–874.

[19] M.S. Islam, M.S. Alam, N. Ghafoori, R. Sadiq, Role of Solution Concentration, cement alkali and test duration on expansion of accelerated mortar bar test, Mater. Struct., 49 (2016) 1955-1965.

[20] P. Rivard, M.A. Berube, J.P. Ollivier, G. Ballivy, Decrease of pore solution alkalinity in concrete tested for alkali-silica reaction, Mater. Struct., 40 (2007) 909-921.

[21] S.U. Einarsdottir, R.D. Hooton, Modifications to ASTM C1293 that Allow Testing of Low Alkali Binder Systems, ACI Mater. J., 115 (2018).

[22] K. Yamada, S. Karasuda, S. Ogawa, Y. Sagawa, M. Osako, H. Hamada, M. Isneini, CPT as an evaluation method of concrete mixture for ASR expansion, Constr. Build. Mater., 64 (2014) 184–191.

[23] M.D.A. Thomas, B. Fournier, K.J. Folliard, M.H. Shehata, Jason H. Ideker, C. Rogers, Performance Limits for Evaluating Supplementary Cementing Materials Using Accelerated Mortar Bar Test, ACI Mater. J., (2007) 115-122.

[24] U. Costa, T. Mangialardi, A.E. Paolini, Minimizing alkali leaching in the concrete prism expansion test at 38°C, Constr. Build. Mater., 146 (2017) 547–554.

[25] T. Chappex, L. Sofia, C. Dunant, K. Scrivener, A Robust Testing Protocol for the Assessment of ASR Reactivity of Concrete, 15th International Conference on Alkali Aggregate Reaction in Concrete (ICAAR) São Paulo Brazil, 2016.

[26] M.D.A. Thomas, Supplementary Cementing Materials in Concrete, Taylor & Francis Group, LLC, Boca Raton, Florida, 2013.

[27] E. Gallucci, X. Zhang, K.L. Scrivener, Effect of temperature on the microstructure of calcium silicate hydrate (C-S-H), Cem. Concr. Res., 53 (2013) 185–195.

[28] K. De Weerdt, M.B. Haha, G. Le Saout, K.O. Kjellsen, H. Justnes, B. Lothenbach, Hydration mechanisms of ternary Portland cements containing limestone powder and fly ash, Cem. Concr. Res., 41 (2011) 279-291.

[29] A. Vollpracht, B. Lothenbach, R. Snellings, J. Haufe, The pore solution of blended cements: a review, Mater. Struct., 49 (2016) 3341–3367.

[30] M.H. Shehata, M.D.A. Thomas, R.F. Bleszynski, The effects of fly ash composition on the chemistry of pore solution in hydrated cement pastes, Cem. Concr. Res., 29 (1999) 1915–1920.

[31] J. Duchesne, M.A. Berube, The Effectiveness of Supplementary Cementing Materials in Suppressing Expansion Due to ASR: Another Look at the Reaction Mechanisms Part 2: Pore Solution Chemistry, Cem. Concr. Res., 24 (1994) 221-230.

[32] T. Chappex, K. Scrivener, Alkali fixation of C–S–H in blended cement pastes and its relation to alkali silica reaction, Cem. Concr. Res., 42 (2012) 1049–1054.

[33] E. L'Hôpital, B. Lothenbach, K. Scrivener, D.A.Kulik, Alkali uptake in calcium alumina silicate hydrate (C-A-S-H), Cem. Concr. Res., 85 (2016) 122–136.

[34] B. Lothenbach, K. Scrivener, R.D. Hooton, Supplementary cementitious materials, Cem. Concr. Res., 41 (2011) 1244–1256.

[35] B. Lothenbach, G.L. Saout, E. Gallucci, K. Scrivener, Influence of limestone on the hydration of Portland cements, Cem. Concr. Res., 38 (2008) 848–860.

[36] M.D.A. Thomas, Field studies of fly ash concrete structures containing reactive aggregates Mag. Concr. Res., 48 (1996) 265-279.

[37] D. Hooton, C. Rogers, C.A. MacDonald, T. Ramlochan, Twenty-Year Field Evaluation of Alkali-Silica Reaction Mitigation, ACI Mater. J., (2013) 539-548.

[38] M.D.A. Thomas, A. Dunster, P. Nixon, B. Blackwell, Effect of fly ash on the expansion of concrete due to alkali-silica reaction – Exposure site studies, Cem. Concr. Compos., 33 (2011) 359–367.

[39] M. Thomas, R.D. Hooton, C. Rogers, B. Fournier, 50 Years Old and Still Going Strong, Concr. Int., (2012) 35-40.

513 [40] A. Leemann, Raman microscopy of alkali-silica reaction (ASR) products formed in concrete, Cem. Concr.
514 Res., 102 (2017) 41–47.
515 [41] A. Leemann, B. Lothenbach, The influence of potassium–sodium ratio in cement on concrete expansion
516 due to alkali-aggregate reaction, Cem. Concr. Res., 38 (2008) 1162–1168.
517 [42] I. Fernandes, Composition of alkali–silica reaction products at different locations within concrete
518 structures, Mater. Charact., 60 (2009) 655-668.
519 [43] A. Leemann, T. Katayama, I. Fernandes, M.A.T.M. Broekmans, Types of alkali–aggregate reactions and the
520 products formed, Constr. Mater., 169 (2016) 128-135.
521 [44] A. Leemann, P. Lura, E-modulus of the alkali–silica-reaction product determined by micro-indentation,
522 Constr. Build. Mater., 44 (2013) 221–227.
523 [45] M.C.G. Juenger, C.P. Ostertag, Alkali–silica reactivity of large silica fume-derived particles, Cem. Concr.
524 Res., 34 (2004) 1389–1402.
525 [46] A. Leemann, C. Merz, An attempt to validate the ultra-accelerated microbar and the concrete
526 performance test with the degree of AAR-induced damage observed in concrete structures, Cem. Concr. Res.,
527 49 (2013) 29–37.
528 [47] N. Thaulow, U.H. Jakobsen, B. Clark, Composition of Alkali Silica Gel and Ettringite in Concrete Railroad
529 Ties: SEM-EDX and X-Ray Diffraction Analyses, Cem. Concr. Res., 26 (1996) 309-318.
530 [48] T. Chappex, K. Scrivener, The influence of aluminium on the dissolution of amorphous silica and its
531 relation to alkali silica reaction, Cem. Concr. Res., 42 (2012) 1645–1649.
532 [49] K.L. Scrivener, P.J.M. Monteiro, The Alkali-Silica Reaction in a Monolithic Opal, J. Am. Ceram. Soc., 77
533 (1994) 2849-2856.
534 [50] Z. Shia, G. Geng, A. Leemann, B. Lothenbach, Synthesis, characterization, and water uptake property of
535 alkali-silica reaction products, Cem. Concr. Res., 121 (2019) 58–71.
536 [51] R. Bleszynski, M. Thomas, Microstructural Studies of Alkali-Silica Reaction in Fly Ash Concrete Immersed in
537 Alkaline Solutions, Adv. Cem. Based Mater., 7 (1998) 66–78.
538 [52] A. Leemann, G.L. Saout, F. Winnefeld, D. Rentsch, B. Lothenbach, Alkali–Silica Reaction: the Influence of
539 Calcium on Silica Dissolution and the Formation of Reaction Products, J. Am. Ceram. Soc., 94 (2011) 1243–1249

[53] R. Taylor, I.G. Richardson, R.M.D. Brydson, Composition and microstructure of 20-year-old ordinary Portland cement–ground granulated blast-furnace slag blends containing 0 to 100% slag, Cem. Concr. Res., 40 (2010) 971–983.

[54] F. Deschner, B. Lothenbach, F. Winnefeld, J. Neubauer, Effect of temperature on the hydration of Portland cement blended with siliceous fly ash, Cem. Concr. Res., 52 (2013) 169-181.

[55] T. Chappex, K. Scrivener, The Effect of Aluminum in Solution on the Dissolution of Amorphous Silica and its Relation to Cementitious Systems, J. Am. Ceram. Soc., 96 (2013) 592-597.

[56] B.R. Bickmore, K.L. Nagy, A.K. Gray, A.R. Brinkerhoff, The effect of $Al(OH)_4^-$ on the dissolution rate of quartz, Geochim. Cosmochim. Acta, 70 (2006) 290–305.

[57] S.-Y. Hong, F.P. Glasser, Alkali binding in cement pastes Part I. The C-S-H phase, Cem. Concr. Res., 29 (1999) 1893–1903.